SPECTROSCOPIC CONFIRMATION OF TWO LYMAN BREAK GALAXIES AT REDSHIFT BEYOND 7

E. Vanzella[1], L. Pentericci[2], A. Fontana[2], A. Grazian[2], M. Castellano[2], K. Boutsia[2], S. Cristiani[1], M. Dickinson[3],
S. Gallozzi[2], E. Giallongo[2], M. Giavalisco[4], R. Maiolino[2], A. Moorwood[5], D. Paris[2], and P. Santini[2]

[1] INAF Osservatorio Astronomico di Trieste, Via G.B. Tiepolo 11, 34131 Trieste, Italy; vanzella@oats.inaf.it
[2] INAF Osservatorio Astronomico di Roma, Via Frascati 33,00040, Monteporzio (RM), Italy
[3] National Optical Astronomy Observatory, P.O. Box 26732, Tucson, AZ 85726, USA
[4] Department of Astronomy, University of Massachusetts, 710 North Pleasant Street, Amherst, MA 01003, USA
[5] European Southern Observatory, Karl-Schwarzschild Strasse, 85748 Garching bei Munchen, Germany

ABSTRACT

We report the spectroscopic confirmation of two Lyman break galaxies at redshift >7. The galaxies were observed as part of an ultra-deep spectroscopic campaign with FORS2 at the ESO/VLT for the confirmation of $z \simeq 7$ "z-band dropout" candidates selected from our VLT/Hawk-I imaging survey. Both galaxies show a prominent emission line at 9735 Å and 9858 Å, respectively: the lines have fluxes of $\sim(1.6–1.2) \times 10^{-17}$ erg s^{-1} cm^{-2} and exhibit a sharp decline on the blue side and a tail on the red side. The asymmetry is quantitatively comparable to the observed asymmetry in $z \sim 6$ Lyα lines, where absorption by neutral hydrogen in the intergalactic medium (IGM) truncates the blue side of the emission-line profile. We carefully evaluate the possibility that the galaxies are instead at lower redshift and we are observing either [O II], [O III], or Hα emission: however from the spectroscopic and the photometric data we conclude that there are no other plausible identifications, except for Lyα at redshift >7, implying that these are two of the most robust redshift determination for galaxies in the reionization epoch. Based on their redshifts and broadband photometry, we derive limits on the star formation rate and on the ultraviolet spectral slopes of the two galaxies. We argue that these two galaxies alone are unlikely to have ionized the IGM in their surroundings.

Key words: galaxies: distances and redshifts – galaxies: formation – galaxies: high-redshift

Online-only material: color figures

1. INTRODUCTION

The recent progress in the exploration of the very early universe has been quite remarkable with several groups beginning to assemble large samples of candidate high-redshift galaxies ($z > 6.5$). These include narrowband-selected Lyα emitters (LAEs; Ota et al. 2010; Ouchi et al. 2010; Hu et al. 2010) and color-selected Lyman break galaxies (LBGs) from wide and deep surveys carried out in the near-IR, mainly with WFC3 (Bouwens et al. 2010a; McLure et al. 2010) and Hawk-I (Castellano et al. 2010a, 2010b, hereafter C10a and C10b, respectively).

Despite the large number of candidates, spectroscopic confirmation of a sizable sample of high-redshift galaxies is still lacking. A systematic spectroscopic follow-up is of paramount importance for three different reasons. First, to evaluate the accuracy and reliability of the Lyman break selection technique that, albeit quite successful at $z \simeq 6$, has never been validated at these extreme redshifts. In addition, the intensity of the Lyα can provide clues on the rest-frame properties of the observed galaxies: knowledge of the exact redshift and the contribution of Lyα and other emission lines to the observed broadband magnitudes are needed to derive the rest-frame properties of the galaxies from the observed continuum (star formation rate (SFR), dust content, metallicity). Finally, and more intriguing, the very visibility of the Lyα and the distribution of its equivalent width (EW) in high-z galaxies can provide useful constrains on the ionization state of the intergalactic medium (IGM) at epochs less than 800 Myr after the big bang (e.g., Fontana et al. 2010, hereafter F10; Ouchi et al. 2010).

To date, only a few galaxies have been confirmed at $z \simeq 7$ or beyond. Following the early identification of the $z = 6.96$ LAE by Iye et al. (2006), a gamma-ray burst host was reported at

$z \simeq 8.1$ by both Salvaterra et al. (2009) and Tanvir et al. (2009), but with considerable uncertainties on the exact redshift, due to the absence of an emission line in the spectra. Very recently the detection of a galaxy at $z = 8.6$ was claimed by Lehnert et al. (2010), although the Lyα emission line in the spectrum has very low signal-to-noise ratio (S/N) and a high uncertainty in the flux calibration.

In this context, we have started a systematic campaign of spectroscopic follow-up of $z \simeq 7$ "z-band dropout" candidates, selected from our imaging survey obtained with VLT/Hawk-I (C10a and C10b). In F10, we presented the results on the sample selected in the GOODS-S field. Out of seven candidates observed, we tentatively detected only one weak Lyα emission line at $z = 6.97$. As discussed in that paper (see also Stark et al. 2010), this very low fraction of confirmations is at odds with what is expected by extrapolating the $z = 5$–6 surveys which detect a much larger fraction of LAEs.

Our survey has continued over the two other fields described in C10b. In this Letter, we present the only two objects with a clear Lyα line at $z \geqslant 7$ found in the entire survey, which are both detected in the BDF4 field (Lehnert & Bremer 2003). The results on the final sample with a full discussion of their implication are deferred to a forthcoming paper (L. Pentericci et al. 2011, in preparation).

All magnitudes are in the AB system, and we adopt $H_0 = 70$ km s^{-1} Mpc^{-1}, $\Omega_M = 0.3$, and $\Omega_\Lambda = 0.7$.

2. TARGET SELECTION AND SPECTROSCOPIC OBSERVATIONS

The targets were selected according to the criteria described extensively in C10b: besides the three z-band dropout candidates
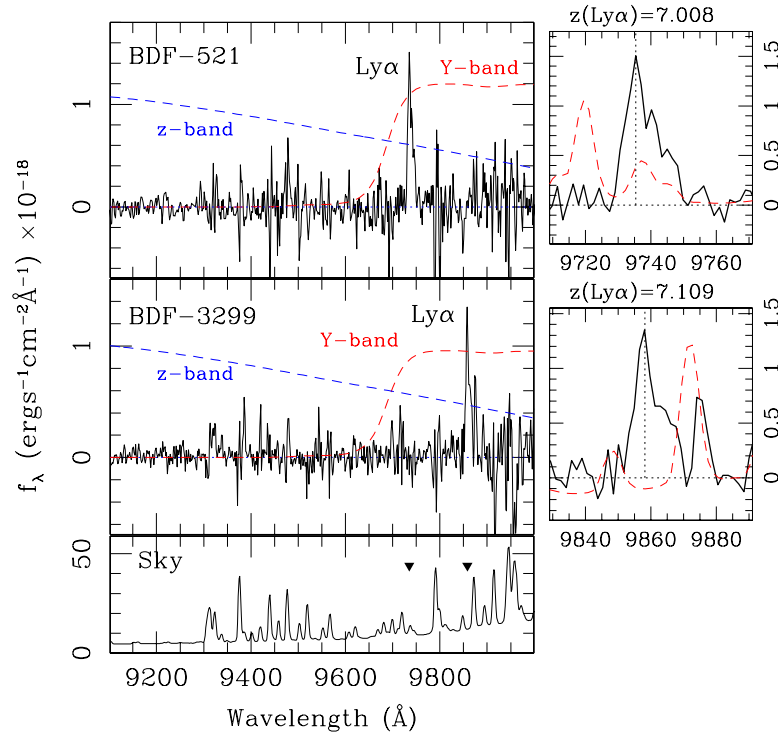
Figure 1. One-dimensional spectra of candidates BDF−521 and BDF−3299. On the left panels spectra are shown with superimposed the *z*-band and *Y*-band filters. In the bottom the one-dimensional (flux calibrated) spectrum of the sky is shown (the position of the Lyα lines is marked with triangles). On the right side the zoomed Lyα lines are shown with the position of the peak marked with a vertical dotted line. The two lines are significant at around 20σ level. In all panels units in the *Y*-axis are 10^{-18} erg s^{-1} cm^{-2} Å^{-1}. The red dashed lines superimposed to the zoomed Lyα (on the right) show the spectrum of the sky in arbitrary units.

(A color version of this figure is available in the online journal.)

listed in Table 3 of that paper, other slits were filled with less secure $z = 7$ candidates as well as *i*-band dropouts.

Observations were taken in service mode with the FORS2 spectrograph on the ESO Very Large Telescope, during 2010 July–August. We used the 600Z holographic grating that provides the highest sensitivity in the range 8000–10000 Å with a spectral resolution $R \simeq 1390$ and a sampling of 1.6 Å pixel^{-1} for a $1'' \times 12''$ slit. The data presented here come from the co-addition of 86 spectra of 665 s of integration each, on a single mask, for a total of 15.9 hr, with median seeing around $0''.8$. Series of spectra were taken at two different positions, offset by $4''$(16 pixels) in the direction perpendicular to the dispersion.

Standard flat-fielding, bias subtraction, and wavelength calibration have been applied as in Vanzella et al. (2009) and F10. The sky background has been subtracted between consecutive exposures, exploiting the fact that the target spectrum is offset due to dithering. Before combining frames, particular care has been devoted to the possible offset along the wavelength direction by measuring the centroids of the sky lines in the wavelength interval 9400–9900 Å. We have also carried out the sky subtraction by fitting a polynomial function to the background. The two approaches provide consistent results.

Finally, spectra were flux calibrated using the observations of spectrophotometric standards. Slit losses are small, given the extremely compact size of the targets, and have been neglected in the subsequent discussion.

3. RESULTS

3.1. Redshift Determination

We detect a prominent emission line in the spectra of two galaxies, candidates BDF−521 and BDF−3299 (C10b) at

wavelengths of 9735 Å and 9858 Å, respectively. In Figures 1 and 2, we present the sky-subtracted extracted one-dimensional spectra and two-dimensional spectra for both objects. No other lines are detected in the rest of the spectra and no continuum is detected for either object. The total line fluxes are $(1.6 \pm 0.16) \times 10^{-17}$ erg s^{-1} cm^{-2} and $(1.2 \pm 0.14) \times 10^{-17}$ erg s^{-1} cm^{-2}, respectively.

Both lines show a clear asymmetric profile with a sharp decline on the blue side and a prominent tail on the red side. This asymmetric profile, which we attribute to absorption by neutral hydrogen, is the best and in many cases unique diagnostic of high-z Lyα emission. Indeed, most LAEs and LBGs at high redshift are too faint to detect the break in the continuum caused by IGM attenuation, with the exception of few very bright objects (Kodaira et al. 2003).

We have investigated the possibility that the lines are instead due to other features, such as Hα, Hβ, [O III]λ5007, or the doublet [O II]$\lambda\lambda$3726 − 3729 in the spectra of lower redshift objects. If the detected emission lines were Hβ or [O III]λ5007 at lower redshift ($z \sim 1.0$ and $\sim$0.95), then both emission lines should be seen in the observed wavelength range. Actually the other component of the [O III] doublet (at λ4959) should also be observed, although with lower S/N. No other lines are detected in the spectra. We also checked that the positions of the expected lines were not coincident with any bright skylines.

In the case of Hα emission from $z \sim 0.50$ galaxies, the rest-frame EW of the line would be exceeding 300 Å, a value that is very rarely observed in star-forming galaxies at low redshift (Salzer et al. 2005). Furthermore, we note that these objects would have a relatively bright continuum also at wavelengths below 1μ and should therefore be observed in the deep *R*, *I*, and *z* bands, where instead we set very stringent upper limits
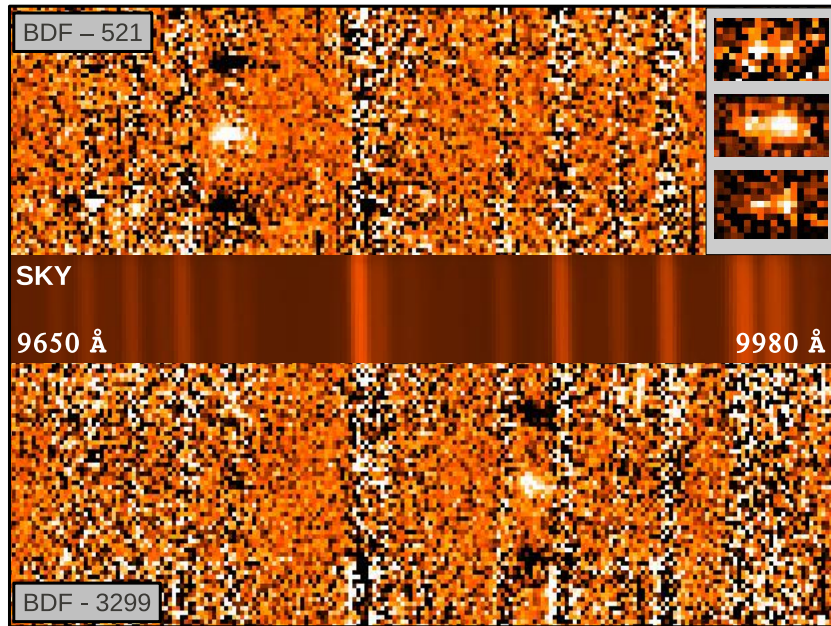
Figure 2. Two-dimensional sky-subtracted spectra of BDF−521 (top) and BDF−3299 (bottom). In both cases the emission line is clearly detected. The "negative" features above and below the emission (typical of the sky subtraction technique) are also evident. In the middle the sky spectrum is shown as a reference for sky line positions. The resolved [O II] doublets at redshift 1.3, 1.5, and 1.6 are shown in the upper right corner, from bottom to top, respectively.

(A color version of this figure is available in the online journal.)

Table 1
Spectroscopic and Photometric Properties of the Two Redshift Seven Galaxies

ID	R.A., Decl. J2000	Redshift	f(Lyα)	SFR(Lyα) $(M_\odot\,yr^{-1})$	EW_{rest} (Å)	FWHM[a] $(km\,s^{-1})$	S_w (Å)	z	Y	J 1σ	K 1σ
BDF−521	336.9444, −35.1188	7.008 ± 0.002	1.62 ± 0.16	8.5	64	240	8.2^{+2}_{-1}	28.00	25.86	>26.5	>26.0
BDF−3299	337.0511, −35.1665	7.109 ± 0.002	1.21 ± 0.14	6.6	50	200	>5.9[b]	>28.55	26.15	>26.5	>26.0

Notes. f(Lyα) in units of $10^{-17}\,erg\,s^{-1}\,cm^{-2}\,\text{Å}^{-1}$.
[a] Measured directly from the line and corrected for instrumental broadening.
[b] This is considered a lower limit since the red side of the emission line is truncated by the presence of a bright skyline (see Figure 1).

for non-detection (AB = 28–29 depending on the band, see Table 1 of C10b).

Finally, in the case of [O II] emitters, the resolution of our spectra ($R = 1390$) would be enough to distinguish the two components of the doublet, which at $z = 1.6$ are separated by 8 Å. We searched for examples in our masks, and we do detect the [O II] doublet in two galaxies at $z \sim 1.6$, one at $z \sim 1.5$ and two at $z \leqslant 1.3$. In particular, the two [O II] at $z \sim 1.6$ fall in the same wavelength region as the lines discussed here and have a lower flux compared to our candidates. In all cases we can clearly distinguish the two components: examples at redshift 1.3, 1.5, and 1.6 are shown in the inset of Figure 2 (top right). Furthermore, we note that typically the [O II] doublet even when unresolved produces an opposite asymmetry with respect to the Lyα shape, because the λ3726 component is often weaker than the λ3729 (see also Rhoads et al. 2003).

Since the correct identification of the line is a critical issue when no other spectral features are present, as mentioned above, the asymmetry can be used to distinguish high-z Lyα emission from foreground [O II], [O III], or Hα emitters (see Stern et al. 2000). To test our ability to recognize asymmetric lines with the S/N of our spectra, we run Monte Carlo simulations by inserting two-dimensional lines of different shapes (Gaussian, truncated Gaussian with variable width, and [O II] doublet with variable ratio of the two components) in the original science

frames at positions corresponding to the observed wavelengths, normalized to the flux of our lines. The frames have been matched in seeing and spectral resolution and reduced as the real ones. This was repeated for all slits where we have no signal detected. We find that an asymmetric line is always recognized as such if it has a width $> 150\,km\,s^{-1}$, and that the [O II] doublet in the one-dimensional spectra is always resolved into two components.

We also calculated the weighted skewness S_w introduced by Shimasaku et al. (2006), to quantify the asymmetry of the two lines. Lyα emission produces always a positive S_w: they set a conservative value of $S_w > 3$ to distinguish LAEs from foreground emitters, although there could be also LAEs with $S_w < 3$. For our two galaxies we find $S_w > 5$–8 (depending on the wavelength's range assumed for the measurement), very similar to the average S_w of $z = 6.6$ LAEs $\langle S_w^{z=6.6}\rangle = 7.31 \pm 1.51$ Å.

We conclude that both lines can be safely identified with Lyα emission: this implies redshifts of 7.008 ± 0.002 and 7.109 ± 0.002 for BDF−521 and BDF−3299, respectively.

3.2. Continuum Fluxes and Spectral Slopes

In the following, we determine the correct UV continuum magnitudes and the Lyα EWs for each object.

1. *BDF−521*. Figure 1 (top panel) shows the relative position of the Lyα line and the two filters Y and z. The IGM opacity affects only 2.7% of the Y-band filter (<0.05 mag for a flat F_ν spectrum), therefore we neglect the IGM attenuation. The observed magnitude is $Y = 25.86 \pm 0.11$, corrected to $Y_{cont} = 26.31$ if the Lyα contribution is subtracted. We note that for this source there is also a 2σ detection at mag 28.00 ± 0.60 in the z-band which is consistent with the Lyα falling at the edge of the z-band filter. Assuming $Y_{cont} = 26.31$ the rest-frame Lyα EW is 64^{+10}_{-9} Å (where the errors come from the line flux uncertainty).

2. *BDF−3299*. The observed magnitude is $Y = 26.15 \pm 0.14$, corrected to $Y_{cont} = 26.58$ if Lyα is subtracted. However, in this case the IGM attenuation affects 15% of the Y-band filter, absorbing completely the continuum blueward of the Lyα line (see Figure 1). Assuming conservatively a flat spectrum for the continuum, we derive $Y_{cont} = 26.40$ and a rest-frame Lyα EW of 50^{+11}_{-8} Å.

Adopting these Lyα EWs we derived the slopes of the UV continuum, fitting to the broadband photometry a set of simple models with flux scaling as $F_\lambda \propto \lambda^\beta$, which include also the Lyα emission and IGM absorption. We derive the best-fit models and the relevant error analysis with a standard χ^2 minimization. The results are shown in Figure 3, where we plot the best-fitting solutions along with the error analysis (see the insets). The best-fit slopes are remarkably steep, with $\beta = -3.7$ and -2.7 for BDF−521 and BDF−3299, respectively, similar to those recently claimed for z-band dropouts on the basis of new *Hubble Space Telescope* (*HST*) WFC3 data ($\beta < -2.5$; Bouwens et al. 2010b; Oesch et al. 2010; Bunker et al. 2010; Finkelstein et al. 2010). However, much shallower solutions with $\beta < -1.7$ and < -0.9 are still allowed at 1σ c.l. ($\Delta\chi^2 = 1$). Clearly, these results are mostly constrained by the non-detection in the J and in the K band (see Table 1).

3.3. Implication for the Stellar Population

We have first explored whether these lines can be ascribed to active galactic nuclei (AGNs). From the non-detection of Nv in the stacked spectrum we derive a 1σ lower limit on the Lyα/Nv > 8. This value is higher than the average ratio for QSOs but not unusual for weak narrow-line AGN found among LBGs (e.g., Steidel et al. 2002), so we cannot exclude this possibility. However, we rely on the fact that AGNs are much rarer than galaxies, and in the following we will assume that the objects are star-forming galaxies.

At the redshifts derived above the implied luminosities for the Lyα lines are 9.3 and 7.3 $\times 10^{42}$ erg s^{-1}. We estimate the SFR from the Lyα luminosity using the Kennicutt's relation (Kennicutt 1998) with the case B recombination theory as SFR $= 9.1 \times L(Ly\alpha)$, with $L(Ly\alpha)$ in units of 10^{43} erg s^{-1}. We obtain values around 7–9 $M_\odot$ yr^{-1} (see Table 1): they represent lower limits since they are not corrected for absorption effects which depend on various parameters, including the neutral fraction of the IGM and the kinematic status of neutral hydrogen within the galaxies (e.g., Ahn 2004).

From the continuum luminosity we obtain $L(UV_{1275}) = 8.1 \times 10^{28}$ and $L(UV_{1260}) = 7.6 \times 10^{28}$ erg s^{-1} Hz^{-1}. We convert luminosities into SFR using the Kennicutt relation for UV continuum, SFR(UV) $= 1.4 \times 10^{-28}L(UV)$. We determine the flux at 1500 Å assuming the slope beta derived before. We obtain SFRs of 8.9 $M_\odot$ yr^{-1} and 9.4 $M_\odot$ yr^{-1}, respectively, similar to those determined from the Lyα line. These values
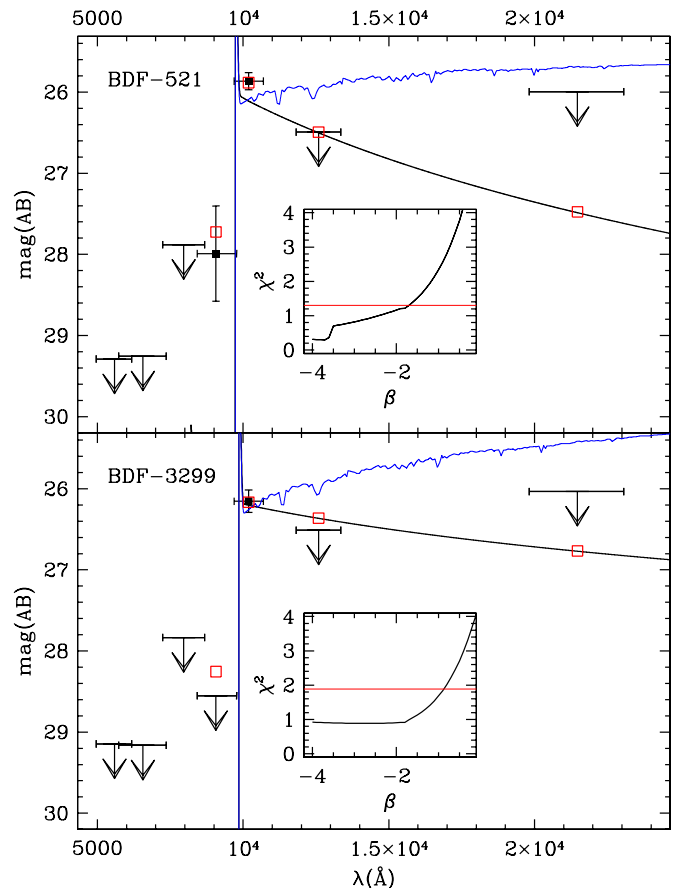

Figure 3. Observed photometry and best-fitting spectral model for BDF−521 (upper panel) and BDF−3299 (lower panel). Black dots and upper limits correspond to observed magnitudes. The solid line is a best-fitting β model. Red dots are the predicted magnitudes from the model. The blue thin line is the dust-extincted Bruzual & Charlot model which provides the maximum SFR with an acceptable χ^2. In the inset the χ^2 as a function of β is shown (the red horizontal line marks the $\Delta\chi^2 = 1$).

(A color version of this figure is available in the online journal.)

are obtained assuming no dust and the agreement of SFR(UV) and SFR(Lyα) is consistent with this scenario. Using instead a global fit to the overall photometry with Bruzual & Charlot templates and a Calzetti et al. (2000) attenuation law, we find best-fit values for SFR that are in excellent agreement with the above determinations, and $E(B - V) = 0$. The standard error analysis on these fits provides the limits one can place on the maximum SFR. Given the poor constraints on the J and K bands, we find that for all models acceptable at 68% confidence level $E(B - V)$ is lower than 0.25–0.35, while the SFRs upper limits are 160 $M_\odot$ yr^{-1} and 400 $M_\odot$ yr^{-1}, respectively, for the two objects, depending on the combination of age and metallicity. Note that the adoption of a Gallerani et al. (2010) attenuation curve would provide an SFR limit about two times lower.

4. DISCUSSION

With the spectroscopic identification of these two $z > 7$ galaxies, we have moved closer to the epoch of reionization and may possibly be observing "re-ionizers" at work at the end of this process. While it is clearly impossible to draw any statistical result out of two objects only, we discuss here a few implications.

Recently, several authors have argued that the fraction of galaxies with large Lyα EW increases in the redshift range

$4 < z < 6$ (e.g., Stark et al. 2010; Douglas et al. 2010; V09). The two emitters reported here with Lyα EW $\geqslant 50$ Å seem to continue this trend. Indeed, the fraction of z-band dropouts spectroscopically confirmed is much higher for this field (two out of three candidates observed), compared to the GOODS-south field (one out of seven candidates; F10).

Therefore, the main results of F10, namely, that the fraction of galaxies with Lyα EW exceeding 50 Å seems to show a sharp decline from $z \sim 6$ to $z \sim 7$, thus reversing the increasing trend from $z \sim 4$ to $z \sim 6$, appear in conflict with the present observations.

However, we anticipate that the result in F10 is confirmed by the analysis of the final sample that includes a third field (L. Pentericci et al. 2011, in preparation) and a much larger statistics. The present spectra indicate that there are considerable field-to-field variations and therefore solid conclusions can be drawn only from large samples.

Turning to the nature of these objects, one can determine whether they are able to ionize the IGM around them. Many models indeed predict that only intrinsically UV bright galaxies have enough photons to build reionized "bubbles" around them, on reasonably short timescales (Dayal et al. 2008). Following Loeb et al. (2005) and assuming SFR of $10\,M_\odot\,\mathrm{yr}^{-1}$ and age 100 Myr, we derive a maximum radius of the H II region of $R_{\mathrm{MAX}} = 0.73(f_{\mathrm{esc}})^{1/3}$ Mpc physical with f_{esc} the fraction of escaping ionizing photons. We are assuming isolated galaxies surrounded by a medium that is mostly neutral when they started to form stars ($z \sim 8$). In order for the Lyα to be transmitted the optical depth τ_{damp} to Lyα absorption at the galaxy redshift has to be less than one (Wyithe & Loeb 2005): this corresponds to an $R = 1.1$ Mpc. Therefore, the radius we have derived would not be large enough even if a maximum $f_{\mathrm{esc}} = 1$ is considered.

As already mentioned the intrinsic SFRs could be considerably higher: for the maximum SFR consistent with our photometry, the galaxies could ionize a large enough region if they had $f_{\mathrm{esc}} > 0.1$. Such values of f_{esc} are not commonly observed in the $z \simeq 3$ universe with few exceptions, such as the compact LBG at $z = 3.8$ recently reported by Vanzella et al. (2010) for which the Lyman continuum ($\lambda < 912$ Å) has been detected directly and whose non-ionizing features reveal $\beta = -2.1$, very weak interstellar absorption lines and absence of Lyα emission.

We stress that with the current depth of the near-infrared observations, it is not possible to produce better constraints on the UV slopes, dust content, and SFR. This issue could easily be solved with a modest investment of *HST* time, by obtaining deep *Y*-, *J*-, and *H*-band WFC3 observations.

If the steep slopes and the dust-free scenarios are confirmed, then the galaxies do not have enough photons to ionize the surrounding H II regions. In such a case, the visibility of the Lyα line in these two objects implies the existence of additional ionizing sources, either galaxies and/or objects of different nature. It is intriguing to surmise that the field-to-field variations in Lyα visibility we observe indicate that the reionization process was very inhomogeneous at these epochs. A possible reason is a clustering effect, particularly efficient since the first objects formed in highly biased regions (e.g., Furlanetto et al. 2006).

We point out that the two confirmed LBGs in the BDF field are at a physical distance from each other that is of the same order as the clustering length of LAEs at $z = 6.6$ $r_0 = 2$–$5h_{100}^{-1}$ Mpc (Ouchi et al. 2010; they are separated by $6'$ in the plane of the sky corresponding to 1.9 Mpc and by 0.101 in redshift space corresponding to a proper distance of 4.4 Mpc). However, there is no evidence of significant enhancement in the density of z-band dropouts in this field.

Another possible mechanism suggested by Wyithe & Loeb (2005) is related to a previous QSO activity, i.e., the H II regions generated by quasars remain as a fossil after the quasar activity ends, since the recombination time is longer than the Hubble time at the mean IGM density for $z < 8$.

These scenarios and their combinations can be tested only when a sizable sample of high-z sources is confirmed and their clustering and physical properties are determined.

REFERENCES

Ahn, S.-H. 2004, ApJ, 601, 25
Bouwens, R. J., et al. 2010a, ApJ, 709, L133
Bouwens, R. J., et al. 2010b, ApJ, 708, L69
Bunker, A. J., et al. 2010, MNRAS, 409, 855
Calzetti, D., Armus, L., Bohlin, R. C., Kinney, A. L., Koornneef, J., & Storchi-Bergmann, T. 2000, ApJ, 533, 682
Castellano, M., et al. 2010a, A&A, 511, A20 (C10a)
Castellano, M., et al. 2010b, A&A, 524, 28 (C10b)
Dayal, P., Ferrara, A., & Gallerani, S. 2008, MNRAS, 389, 1683
Douglas, L. S., Bremer, M. N., Lehnert, M. D., Stanway, E. R., & Milvang-Jensen, B. 2010, MNRAS, 409, 1155
Finkelstein, S. L., Papovich, C., Giavalisco, M., Reddy, N. A., Ferguson, H. C., Koekemoer, A. M., & Dickinson, M. 2010, ApJ, 719, 1250
Fontana, A., et al. 2010, ApJ, 725, L205
Furlanetto, S. R., Zaldarriaga, M., & Hernquist, L. 2006, MNRAS, 365, 1012
Gallerani, S., et al. 2010, A&A, 523, 85
Hu, E. M., Cowie, L. L., Barger, A. J., Capak, P., Kakazu, Y., & Trouille, L. 2010, ApJ, 725, 394
Iye, M., et al. 2006, Nature, 443, 186
Kennicutt, R. C., Jr. 1998, ApJ, 498, 541
Kodaira, K., et al. 2003, PASJ, 55, 17
Lehnert, M. D., & Bremer, M. 2003, ApJ, 593, 630
Lehnert, M. D., et al. 2010, Nature, 467, 940
Loeb, A., Barkana, R., & Hernquist, L. 2005, ApJ, 620, 553
McLure, R. J., Dunlop, J. S., Cirasuolo, M., Koekemoer, A. M, Sabbi, E., Stark, D. P., Targett, T. A., & Ellis, R. S. 2010, MNRAS, 403, 960
Oesch, P. A., et al. 2010, ApJ, 709, L16
Ota, K., et al. 2010, ApJ, 722, 803
Ouchi, M., et al. 2010, ApJ, 723, 869
Rhoads, J. E., et al. 2003, AJ, 125, 1006
Salvaterra, R., et al. 2009, Nature, 461, 1258
Salzer, J. J., Jangren, A., Gronwall, C., Werk, J. K., Chomiuk, L. B., Caperton, K. A., Melbourne, J., & McKinstry, K. 2005, AJ, 130, 2584
Shimasaku, K., et al. 2006, PASJ, 58, 313
Stark, D. P., Ellis, R. S., Chiu, K., Ouchi, M., & Bunker, A. 2010, MNRAS, 408, 1628
Steidel, C. C., Hunt, M. P., Shapley, A. E., Adelberger, K. L., Pettini, M., Dickinson, M., & Giavalisco, M. 2002, ApJ, 576, 653
Stern, D., Bunker, A., Spinrad, H., & Dey, A. 2000, ApJ, 537, 73
Tanvir, N. R., et al. 2009, Nature, 461, 1254
Vanzella, E., et al. 2009, ApJ, 695, 1163 (V09)
Vanzella, E., et al. 2010, ApJ, 725, 1011
Wyithe, J. S. B., & Loeb, A. 2005, ApJ, 625, 1